Mechanism of domain walls drift in pulsed magnetic fields in iron garnet crystals

© *L.A. Pamyatnykh, M.S. Lysov, S.E. Pamyatnykh, L.Yu. Agafonov, D.S. Mekhonoshin, G.A. Shmatov*

Institute of Natural Sciences and Mathematics,
Ural Federal University named after the first President of Russia B.N. Yeltsin,
Ekaterinburg, Russia

E-mail: Lidia.Pamyatnykh@urfu.ru

Conditions for the drift of domain walls in pulsed magnetic fields of various organization (bipolar and unipolar pulsed magnetic fields, pulse packets) are established. Dependences of domain walls drift velocity on the parameters of pulsed magnetic fields (frequency, amplitude, pulse duration) are obtained. As a result of numerical simulation of domain walls drift in a uniaxial sample, an experimentally confirmed mechanism of domain walls drift in pulsed magnetic fields is proposed.

Keywords: pulsed magnetic fields, iron garnets, domain walls, dynamic domain structures, drift of domain walls.

1. Introduction

Controlling the motion of domain walls (DWs) (controlling the magnitude and direction of DW displacement) is a topical problem from the point of view of both fundamental science and possible technical applications [1,2]. Crystals and films of iron garnets are model objects on which new control methods for domain walls can be tested.

The control of DWs using magnetic field is described in a number of works (e.g., [3–6]). It was shown in [7,8] that the direction of displacement of the DWs of a labyrinthine domain structure (DS) in iron garnet films depends on the direction of circular polarization of pulsed laser radiation.

In [9], using the example of large bubble magnetic domains (BMDs) (with the diameter of $50-70\,\mu$m) in Pt/Co/Pt films, the possibility of controlled displacement of domains in the film plane under the action of a pulsed magnetic field without the use of control structures is shown.

From a physical point of view, the displacement of not a single DW, but a system of DWs is of greatest interest. Translational motion of a system of DWs of stripe domains under the action of a harmonic magnetic field (DW drift) was found on silicon iron [10]. Later, the drift of stripe domains was observed in iron garnet plates [11]. In iron garnet films with (210) crystallographic orientation in a unipolar pulsed magnetic field, the drift of lattices of BMDs (LBMD) as well as single-wall S- and L-shaped domains was found [12]. However, the work does not provide information about the quantitative characteristics of the drift motion: the dependence of the drift velocity on the parameters of the pulsed magnetic field. Studies of the drift of DWs of stripe domains in iron garnet crystals in a harmonic magnetic field were continued in [13–16].

In the present work, the conditions for the drift of topologically different DSs (lattices of stripe and bubble domains) in pulsed magnetic fields (PMFs) with varying PMF parameters (frequency, amplitude, pulse duration) are established, and the dependences of the drift velocity of the DWs of stripe domains on the PMF parameters are obtained. Both single pulses and series of pulses (packets of pulses) were applied to the sample. As a result of numerical simulation of DW drift in uniaxial sample in pulsed magnetic field, the DW drift mechanism was proposed, which was then confirmed experimentally.

2. Samples and measurement methods

The magnetic field pulses were formed using flat 100-turn coil with average radius of 10 mm and a current pulse generator through audio-frequency power amplifier. Pulsed magnetic field with frequency f from 0.05 to 500 Hz and amplitudes H_0 up to 370 Oe was applied perpendicular to the sample plane. Dynamic domain structures (DDS) were visualized using the Faraday effect and recorded using a stroboscopic setup based on a pulsed laser with wavelength of 527 nm and pulse duration less than 30 ns.

The laser illumination pulse was applied after the end of impact of each magnetic field pulse. To measure the DW displacements, video recordings obtained using a digital camera were divided into single frames, and a special program was used to monitor the change in the position of each domain wall after the action of a field pulse.

The results obtained at a temperature of $T = 300$ K on a plate cut parallel to the (111) crystallographic plane from $(TbErGd)_3(FeAl)_5O_{12}$ iron garnet single crystal (plate thickness 73 μm, saturation magnetization $M_s = 38$ G, cubic anisotropy constant $K_1 = -3.4 \cdot 10^3$ erg/cm^3, uniaxial
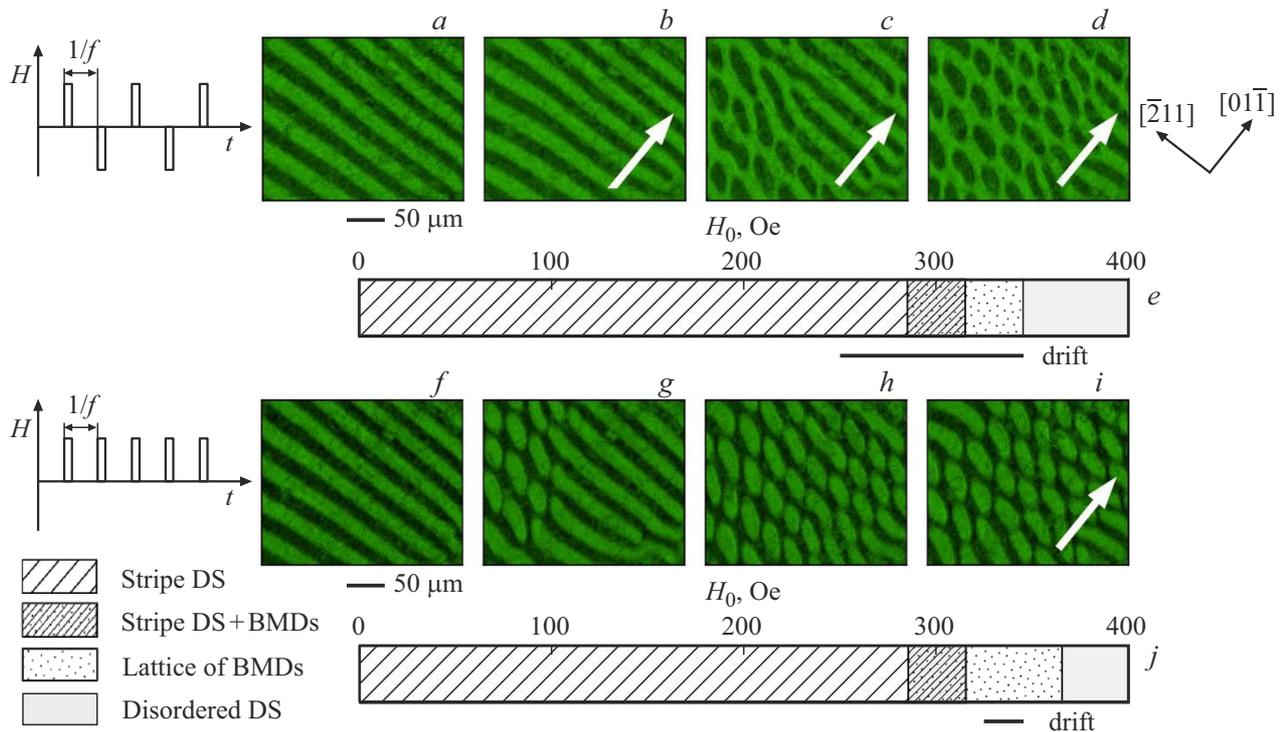
Figure 1. Magneto-optical images of dynamic domain structures emerging in iron garnet plate in a bipolar (a−d) and unipolar (f−i) pulsed magnetic field. Diagrams of types of domain structures depending on the amplitude H_0 of a bipolar (e) and unipolar (j) PMF. Magnetic field pulse frequency $f = 200$ Hz, pulse duration $\tau = 0.2$ ms, pulse field amplitude H_0: a) 0, b) 251, c) 301, d) 315, f) 0, g) 303, h) 319, i) 341 Oe. The arrows show the direction of the drift of the domain structure.

anisotropy constant $K_u = 5.5 \cdot 10^3$ erg/cm³) are presented. The ratio of the magnetic anisotropy constants makes it possible to consider the sample close to uniaxial.

3. Directional motion of DWs in iron garnet crystal in pulsed magnetic fields

The main stages of dynamic magnetization of a uniaxial sample in bipolar and unipolar pulsed magnetic fields are studied. Figure 1 shows images of dynamic domain structures that were formed in a bipolar PMF (Fig. 1, a−d) and a unipolar PMF (Fig. 1, f−i) at pulse frequency $f = 200$ Hz and pulse duration $\tau = 0.2$ ms. The regions of existence of the main types of DDS depending on the field amplitude H_0 are shown in the diagrams for bipolar (Fig. 1, e) and unipolar (Fig. 1, j) PMF.

In the initial demagnetized state, stripe DS was observed in the sample, in which the DWs were oriented along the $[\bar{2}11]$ axis (Fig. 1, a and Fig. 1, f).

The state of the crystal after „shaking" in an alternating magnetic field with a frequency $f = 50$ Hz and amplitude decreasing from the saturation field amplitude to zero was taken as the demagnetized state. In a bipolar PMF with an amplitude $H_0 < 250$ Oe oscillations of the DWs are observed in the sample while DW orientation remains

unchanged. In the field $H_0 = 250$ Oe stripe domains start to drift in the direction of the $[01\bar{1}]$ axis perpendicular to the DWs. At that the orientation of the DWs and the period of the stripe DS do not change (Fig. 1, b, here and below, the direction of the drift is shown by an arrow). When the PMF amplitude reaches $H_0 = 285$ Oe, the stripe domains are broken and elliptical BMDs are formed (Fig. 1, c), which drift together with the stripe domains. In the course of the drift a reorientation of the BMDs is observed: the major axis of the elliptical BMDs rotates from the $[\bar{2}11]$ axis by an angle of about 30° practically to the $[\bar{1}10]$ axis. The lattice of elliptical BMDs formed in the field $H_0 = 315$ Oe (Fig. 1, d) drifts in the direction $[01\bar{1}]$. It has been established that DDS drift takes place in the amplitude range $H_0 = 250-345$ Oe, in which the stripe domain structure and lattice of elliptical BMDs exist in the sample. The drift termination is associated with the destruction of the ordered domain structure in the sample, when the nature of the displacement of the domain walls changes from an ordered unidirectional motion to a disordered chaotic displacement of DWs.

Similar transformation of the DDS is observed in a unipolar PMF. The stripe domains aligned along the $[\bar{2}11]$ axis are broken and elliptical BMDs are formed, which are rearranged in the field in such a way that the major axis of the elliptical BMDs is oriented along the $[\bar{1}10]$ axis, which makes an angle close to 30° with the orientation of

the stripe domains. The lattice of elliptical BMDs formed in the field $H_0 = 319$ Oe (Fig. 1,h) does not drift. The LBMD drift starts at $H_0 > 339$ Oe and continues up to $H_0 = 360$Oe, when the ordered movement of the BMDs changes into the disordered motion of the DDS. In contrast to the behavior of DDS in a bipolar PMF, in a unipolar pulsed field the DS drift occurs only for the BMD lattice and starts at field amplitudes at which the LBMD drift in a bipolar PMF is already over. In this case, the direction of the DS drift does not depend on the PMF polarity and coincides with the direction of the drift in a bipolar PMF.

Thus, in bipolar PMF, the drift of topologically different DDSs (stripe domains and lattices of elliptical BMDs) is observed in a fairly wide range of amplitudes $250-345$ Oe (shown as a black line in the diagram in Fig. 1,e). In a unipolar PMF, regardless of the polarity of the pulses, only elliptical BMD lattices drift in a small amplitude range of $339-360$ Oe (shown as a black line in Fig. 1,j). In this case, the direction of DDS drift does not depend on the PMF configuration.

4. Dependence of domain walls drift velocity on parameters of bipolar pulsed magnetic field

Figure 2 shows the dependences of the DW drift velocity of stripe domains on the amplitude of the bipolar pulsed magnetic field in the range of pulse frequencies $f = 30-500$ Hz and amplitudes $H_0 = 240-310$ Oe. In the pulse frequency range studied, the drift velocity increases with the increase in the PMF amplitude. Moreover, at PMF amplitudes in the interval of $240-260$ Oe, the drift velocity V_{dr} increases linearly, then up to $H_0 = 280$ Oe V_{dr} practically does not change, and at amplitudes $H_0 > 285-290$ Oe, a sharp increase in the drift velocity is observed, which corresponds to the beginning of the BMD formation region (see the diagram in Fig. 1,e). In this case, the dependences of the DW drift velocity on the field amplitude have the form of quadratic functions. At fixed amplitude the drift velocity increases linearly with the increase of frequency of applied magnetic field pulses (see inset in Fig. 2).

Figure 3 shows the dependence of the DW drift velocity on the pulse duration τ in the range of $2.1-5.1$ ms. It can be seen that the drift velocity increases with increase in the duration of the magnetic field pulses, and the dependence is close to linear.

It should be noted that the absolute values of the DW drift velocity in this sample in pulsed magnetic field are an order of magnitude lower than the typical values of the drift velocity in harmonic magnetic field at comparable values of the field frequency and amplitude [13]. In harmonic magnetic field, the maximum values of the DW drift velocity in the frequency range of $75-1200$ Hz are $0.5-2.0$ mm/s, respectively. The difference in the absolute values of the drift velocity is due to the fact that in the case of PMF the
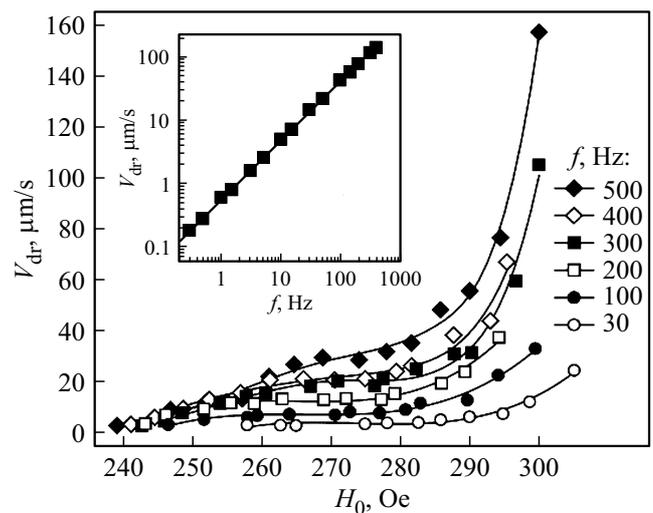

Figure 2. Dependences of the DW drift velocity on the amplitude of the bipolar PMF in the frequency range $f = 30-500$ Hz; the inset shows the dependence of the DW drift velocity on the PMF frequency at the amplitude $H_0 = 300$ Oe.
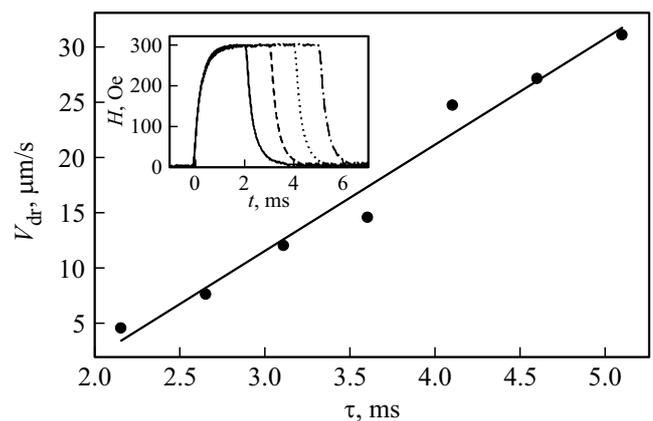

Figure 3. Dependence of DW drift velocity on the duration of bipolar PMF pulses ($H_0 = 300$ Oe, $f = 30$ Hz); the insert shows the shape of the applied pulses (duration $\tau = 2.1, 3.1, 4.1, 5.1$ ms).

domain wall moves only during a small part of the magnetic field period. At the same time, many regularities of DW drift motion are common for PMF and harmonic magnetic field: the threshold nature of the drift, the increase in the drift velocity with increase in the frequency and amplitude of the field.

5. Response of the DW system to the impact of sequences (packets) of magnetic field pulses

The response of a system of stripe domains during the transition from bipolar PMF to unipolar PMF has been studied. The studies were performed using two experimental schemes. In the first scheme, the transition
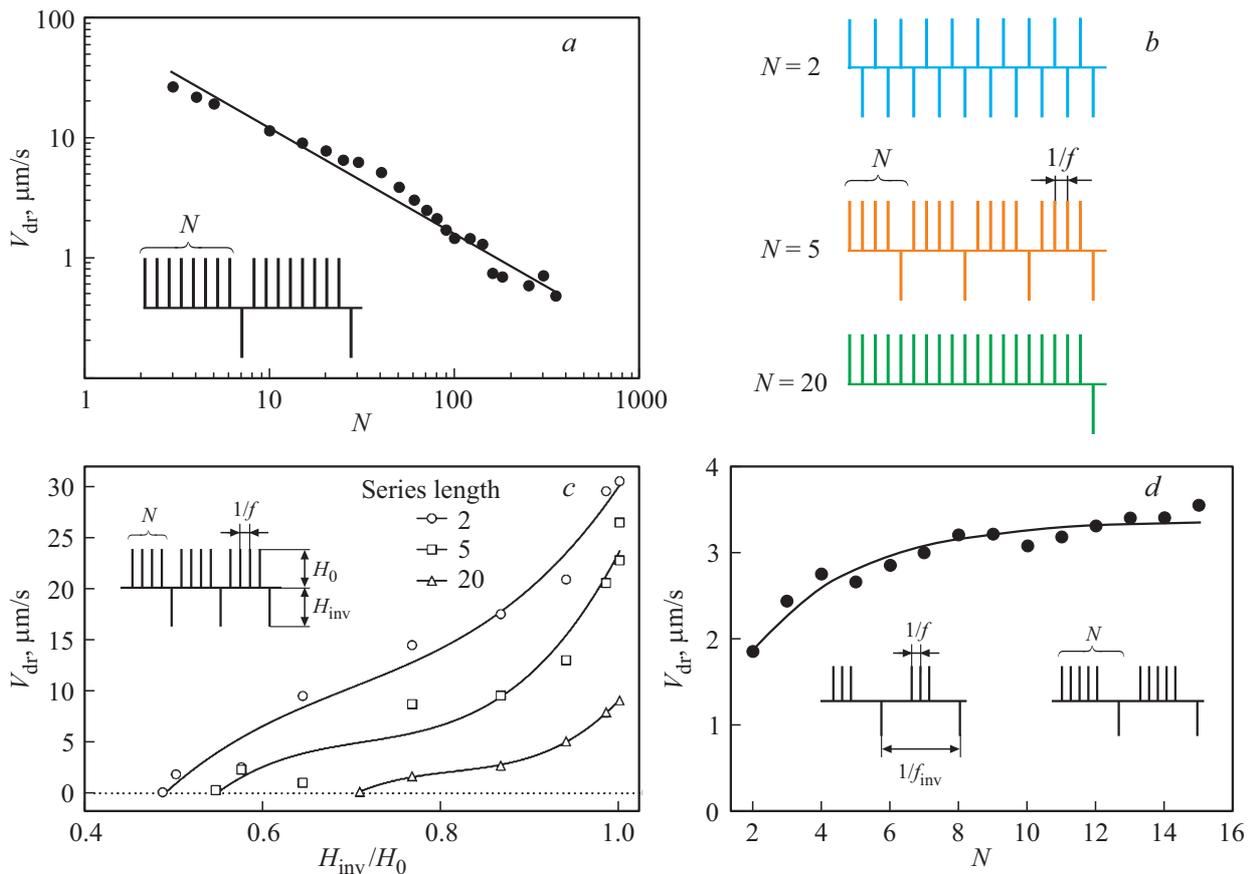
Figure 4. *a*) The dependence of the drift velocity V_{dr} on the number of pulses N in a packet at $H_{inv} = H_0 = 300$ Oe, the frequency of field pulses $f = 200$ Hz. *b*) Diagrams of pulse series for $N = 2, 5, 20$. *c*) Dependencies of the drift velocity V_{dr} on the ratio H_{inv}/H_0 for pulse packets at $N = 2, 5, 20$ ($H_0 = 305$ Oe, $f = 200$ Hz). *d*) The dependence of the DW drift velocity on the number of pulses in the packet ($f_{inv} = 5$ Hz, $f = 100$ Hz, pulse amplitude $H_0 = 305$ Oe, pulse duration $\tau = 3.1$ ms).

was carried out by reducing the frequency of pulses of one of the polarities of the bipolar PMF, the pulses were applied in repetitive packets of N pulses, where $N - 1$ sequential pulse had positive polarity and amplitude H_0, and one pulse had negative polarity and amplitude $H_{inv} = H_0$. The form of the pulse packet for an arbitrary N is shown in the inset in Fig. 4, *a*; the form of pulse packets for $N = 2, 5, 20$ is shown in Fig. 4, *b*. When a sample is exposed to sequences (packets) of magnetic field pulses, the nature of the drift of stripe DDS is similar to that described in Section 3 for the case of bipolar PMF. Figure 4, *a* shows the dependence of the DW drift velocity of stripe domains on the total number of pulses in packets $H_{inv} = H_0 = 300$ Oe and the field pulse frequency $f = 200$ Hz. It can be seen that the drift velocity increases with decreasing N (i.e. the number of pulses in the packet) and is maximum at $N = 2$.

In the second experimental scheme $N - 1$ pulse of positive polarity had the same amplitude H_0, while the amplitude of the negative pulse H_{inv} varied from the positive polarity pulse amplitude H_0 to 0 at a fixed pulse repetition frequency. Figure 4, *c* shows the DW drift velocity at $H_0 = 305$ Oe and pulse frequency $f = 200$ Hz depending on the ratio of the negative pulse amplitude to amplitude of

pulses of positive polarity H_{inv}/H_0 for a different number of pulses N in a packet. It can be seen that the amplitude of the negative pulse required to start the drift is the higher, the less often this pulse is applied; the drift velocity increases with an increase in the amplitude of the negative pulse at a fixed value of the amplitude of the pulses of positive polarity H_0. At fixed ratio H_{inv}/H_0, the drift velocity increases with the frequency of negative pulses and is maximal at $N = 2$.

Figure 4, *d* illustrates the effect of increase in the number of successively applied pulses of one of the polarities on the velocity of drift of DWs of stripe domains while maintaining the frequency of supply of pulses of reverse polarity. The packet of pulses included $N - 1$ pulse of positive polarity with amplitude H_0 and one pulse of negative polarity with amplitude $H_{inv} = H_0$ on time interval $1/f_{inv}$, organized as shown in the insert in Fig. 4, *d*. The number of pulses in a packet was varied from 2 to 20, the frequency of pulses of positive polarity was $f = 100$ Hz, the frequency of pulses of negative polarity was $f_{inv} = 5$ Hz. It can be seen in Fig. 4, *d* that increase in the number of pulses of positive polarity leads to increase in the drift velocity, then the drift velocity of the DWs reaches to saturation at $N \approx 8$.
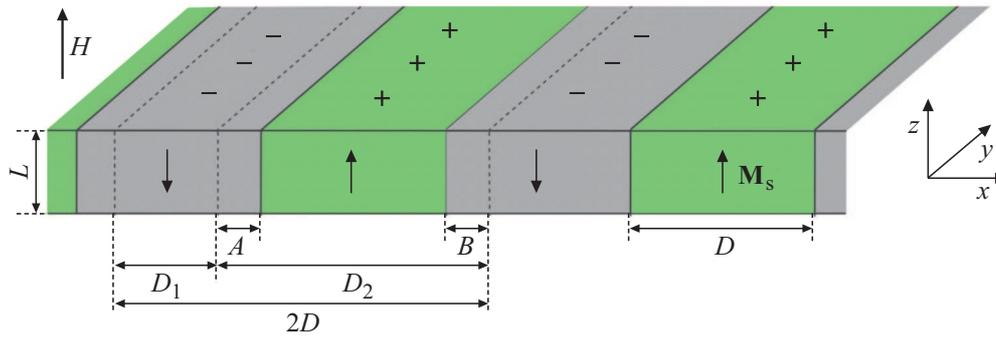
Figure 5. Model of stripe domain structure.

6. Numerical simulation of DW motion in pulsed magnetic field

Numerical simulation of DW motion in a uniaxial iron garnet crystal in bipolar pulsed magnetic field was performed using the coupled oscillators model [13,14,17] with the parameters of real samples. Within the framework of this model it is assumed that the internal structure of DWs does not change during motion, DWs have an effective mass and move under the action of pressure forces acting on their surface.

Figure 5 shows the model of stripe domain structure in a magnetically uniaxial iron garnet plate with thickness L. The easy magnetization axis is perpendicular to the plane of the plate and parallel to the OZ axis. The magnetization vectors $\mathbf{M}_s$ in the domains are directed parallel to the OZ axis. The width of stripe domains D in the absence of an external magnetic field was determined experimentally. The period of the domain structure is equal to twice the domain width $2D$.

External periodic bipolar pulsed magnetic field was applied perpendicular to the sample plane. In this case, the following forces act on the DWs: the force from the external magnetic field, leading to the displacement of the DWs from the equilibrium position, the „restoring" force associated with the magnetostatic energy of the stripe domain structure, and the dynamic friction force associated with attenuation of the magnetization precession in magnetic field. The coercivity of the DWs is not taken into account in this work.

Denote the displacements of domain walls from the position occupied by them in the absence of a magnetic field as A and B (Fig. 5). These displacements are the same for all periods of the domain structure. In this case, the width of neighboring domains is equal to: $D_1 = D - A - B$ and $D_2 = D + A + B$.

In [13] it was established that when pulses of the field of opposite polarities are applied, the displacement of the DWs in the direction of the drift significantly exceeds the displacement of the DWs in the direction opposite to the drift. The observed difference in the magnitude of the displacements and, consequently, in the velocities of the domain walls can be associated with different values of the attenuation parameter when the DWs move in the direction of the observed drift and in the direction opposite to the drift.

Within the framework of the proposed model, we consider the motion of stripe domain structure in bipolar pulsed magnetic field under the assumption that the attenuation parameter [18–21] is anisotropic with respect to the direction: the values of the attenuation parameter are different when the DWs move in different directions along the axis perpendicular to the domain walls plane. Taking into account the symmetry of the problem, we can write the motion equations for two adjacent domain walls in a pulsed magnetic field, which is sufficient to describe the motion of all DWs in the considered model of the domain structure [13,22].

When passing to dimensionless variables, the equations of motion of the DWs will have the following form:

$$
\begin{cases}
\dfrac{\partial^2 a}{\partial \tau^2} + \eta\left(\mathrm{sgn}\left(\dfrac{\partial a}{\partial \tau}\right)\right)\dfrac{\partial a}{\partial \tau} + g(a,b) - \pi h_0 \tilde{h}(\nu\tau) = 0, \\[2mm]
\dfrac{\partial^2 b}{\partial \tau^2} + \eta\left(-\mathrm{sgn}\left(\dfrac{\partial b}{\partial \tau}\right)\right)\dfrac{\partial b}{\partial \tau} + g(a,b) - \pi h_0 \tilde{h}(\nu\tau) = 0.
\end{cases}
$$
(1)

Here $a = 2\pi A/D$ and $b = 2\pi B/D$ are dimensionless variables corresponding to displacements of two adjacent domain walls from the equilibrium position under the action of pulses of external magnetic field,

$$
g(a,b) = \frac{a+b}{2} + \frac{2}{\ell}\sum_{n=1}^{\infty}\left[\frac{(-1)^n}{n^2}\left[1 - \exp(-n\ell)\sin\frac{n(a+b)}{2}\right]\right],
$$

$\ell = 2\pi L/D$, L is sample thickness, D is the width of one domain in the absence of external magnetic field, m is the DW effective mass, $\Omega^2 = 8\pi M_s^2/mD$, $\tau = t\Omega$, $\nu = 1/\Omega$, h_0 is normalized amplitude of external magnetic field pulses, $\tilde{h}$ is the function of external magnetic field profile.

The attenuation function $\eta(q)$ sets the value of the attenuation parameter depending on the direction of motion of the DWs:

$$\eta(q) = \begin{cases} \eta_1, & q > 0, \\ \eta_2, & q < 0, \end{cases} \qquad (2)$$

where $\eta_i = \alpha_i \left(D(\tilde{A}/K_u)^{-1/2}\right)^{1/2}$ are the values of normalized attenuation parameters, α_i are the values of the Hilbert damping parameter, typical for given materials ($i = 1, 2$) [23], $\tilde{A} \approx 10^{-7}$ erg/cm is the exchange interaction parameter, K_u is the uniaxial anisotropy constant.

System (1) was solved using Wolfram Mathematica © software system (LSODA solver [24]) with homogeneous initial conditions.

Simulations show that even a small difference in the values of the attenuation parameter when the DWs move in opposite directions is sufficient to cause the DWs drift. The difference of the order of 4% is sufficient for DW drift with the maximum velocities observed experimentally (see Section 4). As a result of simulations, the dependences of the drift velocity on the amplitude and frequency of the bipolar pulsed magnetic field are obtained, which, similarly to the corresponding dependences obtained as a result of numerical simulations for the harmonic field [13], are increasing functions of the amplitude and frequency.

The results of numerical simulations are illustrated by the diagram in Fig. 6, which shows the motion of DWs in a bipolar pulsed magnetic field with alternating pulses of different polarities. The equilibrium positions to which the DWs return in the model after the action of field pulses of different polarities are shifted each time by a fixed value Δx in the direction of the DW drift, regardless of the polarity of the field pulse.

Figure 7 shows the time dependences of the coordinates of the equilibrium positions to which the domain walls
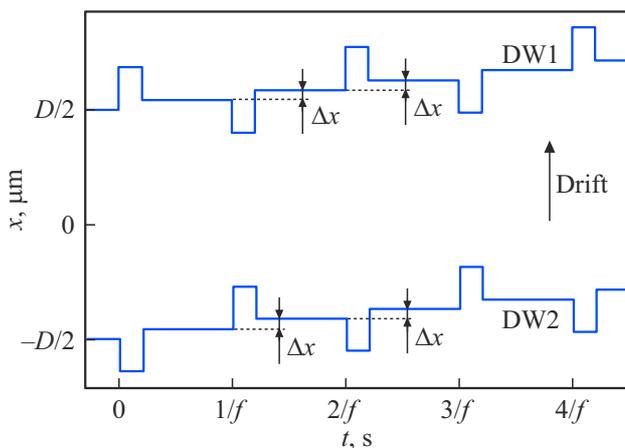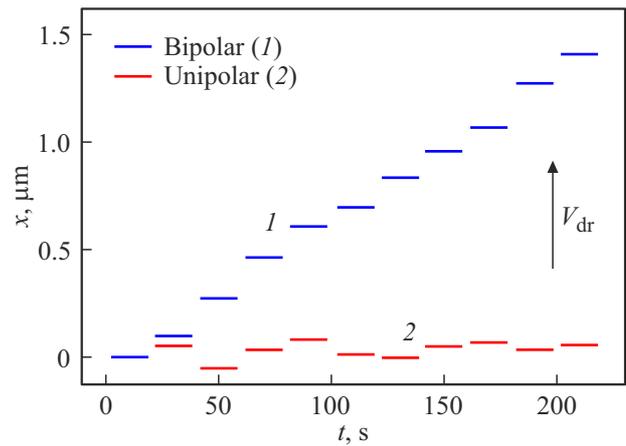

Figure 7. Time dependences of the coordinates of the DW equilibrium positions after the action of a field pulse (experimental data). Blue segments (*1*) are DW positions after exposure to bipolar field pulses. Red segments (*2*) are DW positions after exposure to unipolar field pulses. Pulse repetition frequency $f = 0.05\,\text{Hz}$, rectangular pulse duration is $10\,\text{ms}$.

return after the impact of a field pulse on them, that are obtained experimentally for the iron garnet sample described in Section 2. It can be seen in Fig. 7 that the displacements of the equilibrium positions of the DWs in the bipolar pulsed field towards the drift of the DW are of a fairly regular stepwise nature. At the same time, in a unipolar field, no displacement of the DW equilibrium positions is observed: the DWs remain in the neighborhood of their original position.

Thus, it has been established that the DW drift in bipolar pulsed magnetic field occurs stepwise, by shifting the equilibrium positions of the domain wall system by a small fixed value in the drift direction as a result of the influence of each field pulse, regardless of its polarity.

The diagram of stepped DW motion (Fig. 6) obtained as a result of numerical simulations in bipolar pulsed magnetic field is confirmed experimentally on the real sample with predominant uniaxial anisotropy (Fig. 7).

The results obtained make it possible to control the motion of the system of domain walls by applying pulsed magnetic fields, namely, to position with high accuracy the system of domain walls of a sample in which the drift of the domain structure takes place.

7. Conclusion

The conditions for the existence of the drift of topologically different dynamic DSs (lattices of stripe and bubble domains) in a sample with uniaxial anisotropy in pulsed magnetic fields of various configuration are established. The dependences of the drift velocity of the domain walls of laminar domains on the parameters of the pulsed magnetic field (the amplitude, frequency, and duration of the pulses) are obtained.

Figure 6. Diagram of DW motion in bipolar pulsed magnetic field (results of numerical simulations). Curves DW1 and DW2 correspond to the positions of neighboring DWs at time moments t, $2D$ is the period of the structure, f is the repetition frequency of the field pulses. The arrow indicates the direction of DWs drift.

The response of a system of stripe domains during the transition from bipolar PMF to unipolar PMF was studied by using pulse packets of various organization. The conditions for the appearance of the DW drift depending on the amplitude and frequency of the pulses of the field of reverse polarity are established.

As a result of numerical simulations of DW motion in bipolar pulsed magnetic fields, a diagram of domain walls movement by shifting of the DWs equilibrium positions in the direction of the drift was obtained. This DW drift mechanism is consistent with the experimentally observed DW motion. It has been experimentally established that the DW drift in a bipolar pulsed magnetic field occurs by shifting the equilibrium positions to which the DWs return after exposure to the of field pulses. The displacement of the DWs in the direction of the drift is of a stepwise nature: after each pulse of the field of alternating polarities the equilibrium position shifts in the direction of the drift regardless of the polarity of the magnetic field pulse.

The established mechanism of DW drift in PMF makes it possible to control the motion of DWs in samples with drift of the domain structure: the system of domain walls of the sample can be positioned with high accuracy by applying magnetic field pulses to the sample.

Funding

Conflict of interest

The authors declare that they have no conflict of interest.

References

[1] S.S.P. Parkin, M. Hayashi, L. Thomas. Science **320**, *5873*, 190 (2008).

[2] K.W. Moon, D.H. Kim, S.C. Yoo, S.G. Je, B.S. Chun, W. Kim, B.C. Min, C. Hwang, S.B. Choe. Sci. Rep. **5**, 9166 (2015).

[3] V.G. Baryakhtar, A.N. Bogdanov, D.A. Yablonsky. UFN **156**, *1*, 47 (1988) (in Russian).

[4] A. Hubert, R. Schäfer. Magnetic domains: the analysis of magnetic microstructures. Springer Science & Business Media, Berlin (2008). 696 c.

[5] A.P. Malozemoff, J.C. Slonczewski. Magnetic Domain Walls in Bubble Materials. Advances in Materials and Device Research. Academic Press, N.Y. (2016). 334 p.

[6] D. Sander, S.O. Valenzuela, D. Makarov, C.H. Marrows, E.E. Fullerton, P. Fischer, J. McCord, P. Vavassori, S. Mangin, P. Pirro, B. Hillebrands, A.D. Kent, T. Jungwirth, O. Gutfleisch, C.G. Kim, A. Berger. J. Phys. D **50**, *3*, 363001 (2017).

[7] M.V. Gerasimov, M.V. Logunov, A.V. Spirin, Y.N. Nozdrin, I.D. Tokman. Phys. Rev. B **94**, *1*, 014434 (2016).

[8] S.A. Nikitov, A.R. Safin, D.V. Kalyabin, A.V. Sadovnikov, E.N. Beginin, M.V. Logunov, M.A. Morozova, S.A. Odintsov, S.A. Osokin, A.Yu. Sharaevskaya, Yu.P. Sharaevskiy, A.I. Kirilyuk. UFN **190**, *10*, 1009 (2020) (in Russian).

[9] D. Petit, P.R. Seem, M. Tillette, R. Mansell, R.P. Cowburn. Appl. Phys. Lett. **106**, *2*, 022402 (2015).

[10] B. Passon. Zeitschrift für Angewandte Physik **25**, *2*, 56 (1968).

[11] V.K. Vlasko-Vlasov, L.S. Uspenskaya. ZhETF **91**, *4*, 1483 (1986) (in Russian).

[12] F.V. Lisovsky, E.G. Mansvetova, Ch.M. Pak. ZhETF **108**, *3*, 1031 (1995) (in Russian).

[13] L.A. Pamyatnykh, D.S. Mekhonoshin, S.E. Pamyatnykh, L.Yu. Agafonov, M.S. Lysov, G.A. Shmatov. FTT **61**, *3*, 483 (2019) (in Russian).

[14] L.A. Pamyatnykh, G.A. Shmatov, S.E. Pamyatnykh, M.S. Lysov, D.S. Mekhonoshin, A.V. Druzhinin. Acta Phys. Pol. A **127**, *2*, 388 (2015).

[15] L.A. Pamyatnykh, B.N. Filippov, L.Y. Agafonov, M.S. Lysov. Sci. Rep. **7**, 18084 (2017).

[16] L. Pamyatnykh, M. Lysov, S. Pamyatnykh, G. Shmatov. JMMM **542**, 168561 (2022)

[17] S. Chikazumi. Physics of Ferromagnetism. Oxford University Press, N.Y. (2009). 668 p.

[18] V.V. Randoshkin, Yu.N. Sazhin. ZhTF **66**, *8*, 83 (1996) (in Russian).

[19] A.V. Kobelev, Yu.N. Shvachko, V.V. Ustinov. FMM **117**, *1*, 11 (2016) (in Russian).

[20] K. Gilmore, M.D. Stiles. Phys. Rev. B **81**, *17*, 174414 (2010).

[21] I.P. Miranda, A.B. Klautau, A. Bergman, D. Thonig, H.M. Petrilli, O. Eriksson. Phys. Rev. B **103**, L220405 (2021).

[22] G.S. Kandaurova, L.G. Onoprienko. Osnovnyye voprosy teorii magnitnoy domennoy struktury. UrGU, Sverdlovsk (1977). 124 p. (in Russian).

[23] Yu.M. Yakovlev, S.Sh. Gendelev. Monokristally ferritov v radioelektronike. Sov. Radio, M. (1975). 360 p. (in Russian).

[24] A.C. Hindmarsh. IMACS Transac. Sci. Comput. **1**, 55 (1983).